Hydrology and
Earth System
Sciences
Discussions

Open Access

Assimilation of surface soil moisture into a multilayer soil model: design and evaluation at local scale

M. Parrens, J.-F. Mahfouf, A. Barbu, and J.-C. Calvet

CNRM-GAME, UMR3589, Météo-France, CNRS, Toulouse, France

Correspondence to: J.-C. Calvet (jean-christophe.calvet@meteo.fr)

Discussion Paper | Discussion Paper | Discussion Paper | Discussion Paper |

HESSD

10, 9645–9688, 2013

Design and evaluation at local scale

M. Parrens et al.

Title Page

Abstract | Introduction

Conclusions | References

Tables | Figures

◀ | ▶

◀ | ▶

Back | Close

Full Screen / Esc

Printer-friendly Version

Interactive Discussion

Abstract

Land surface models (LSM) have improved considerably in the last two decades. In this study, the ISBA LSM soil diffusion scheme is used (with 11 soil layers represented). A Simplified Extended Kalman Filter (SEKF) allows surface soil moisture (SSM) to be assimilated in the multi-layer LSM in order to constrain deep soil moisture. In parallel, the same simulations are performed using the ISBA LSM with 2 soil layers (a thin surface layer and a bulk reservoir). Simulations are performed over a 3 yr period (2003–2005) for a bare soil field in southwestern France, at the SMOSREX experimental site. Analyzed soil moisture values correlate better with soil moisture observations when the ISBA LSM soil diffusion scheme is used. The Kalman gain is greater from the surface to 45 cm than below this limit. For dry periods, corrections introduced by the assimilation scheme mainly affect the first 25 cm of soil whereas weaker corrections impact the total soil column for wet periods. Such seasonal corrections cannot be described by the two-layer ISBA LSM. Sensitivity studies performed with the multi-layer LSM show improved results when SSM (0–6 cm) is assimilated into the second layer (1–5 cm) than into the first layer (0–1 cm). The introduction of vertical correlations in the background error covariance matrix is also encouraging. Using a yearly CDF-matching scheme for bias correction instead of matching over the three years permits the seasonal variability of the soil moisture content to be better transcribed. An assimilation experiment has also been performed by forcing ISBA-DF with a local forcing setting precipitation to zero. This experiment shows the benefit of the SSM assimilation for correcting inaccurate atmospheric forcing.

1 Introduction

It is well known that land surface processes interact strongly with the lower boundary of the atmosphere. In climate and numerical weather prediction (NWP) models, surface-interaction processes are represented by land surface models (LSMs). LSMs

determine the partitioning of surface energy between sensible and latent heat fluxes, which depend on the quantity of water available in the root-zone (Shukla and Mintz, 1982; Koster and Suarez, 1995; Entekhabi et al., 1999). The characterization of soil moisture in deep layers is more important than for surface soil moisture as the su-
5 perficial reservoir has a small capacity and no memory features. Accurate estimates of root-zone soil moisture are also important for many applications in hydrology and agriculture. Therefore, the land dynamics needs to be sufficiently accurate. For example, a finer discretization in the vertical soil moisture and temperature profiles allows for a much better description of the nonlinear behavior than two-layer or three-layer
10 models can provide (Reichle, 2000).

Considerable improvements have been made to the initial state of LSMs during the last decade by assimilating remotely sensed near-surface soil moisture data (Houser et al., 1998; Crow and Wood, 2003; Reichle and Koster, 2005; Balsamo et al., 2007). Interest in this was motivated by recent advances in soil moisture remote sensing. Since
15 the 1970s, remote sensing has come to be accepted as a potential tool to access soil moisture at different temporal and spatial scales. Schmugge (1983) shows that the low-frequency microwave range is suitable for measuring the water content of a shallow, near-surface layer. Numerous missions to map surface soil moisture globally have been launched, such as ASCAT (Advanced Scatterometer onboard METOP, Wagner
20 et al., 2007), the Advanced Microwave Scanning Radiometer EOS (AMSR-E) sensor (Njoku et al., 2003), and the Soil Moisture and Ocean Salinity (SMOS) satellite (Kerr et al., 2001), or are scheduled for launch (Soil Moisture Active Passive (SMAP) satellite Entekhabi et al., 2004). Moreover, the development of soil moisture retrieval algorithms for pre-existing microwave remote sensing missions (Wagner et al., 1999; Owe et al.,
25 2001; Bartalis et al., 2007) offers an opportunity to improve the realism of modeled soil moisture. Several authors (Entekhabi et al., 1994; Houser et al., 1998; Walker and Houser, 2001; Ragab, 1995; Sabater et al., 2007 among others) have shown that combining SSM measured by remote sensing and LSM simulations through a Land Data Assimilation System (LDAS) improves the modeled soil moisture content for deep

Design and evaluation at local scale

M. Parrens et al.

layers. However, there are considerable uncertainties associated with the use of remotely sensed soil moisture data. In particular, the extent to which the near-surface soil layer represents the underlying soil moisture profile is not well understood.

Satellite data have to be calibrated and validated by observations in situ. The SMOSREX experimental site located in southwestern France was used for the algorithm validation of SMOS (Saleh et al., 2006, 2007). Over this site, measurements of soil moisture and temperature profiles, meteorological variables and brightness temperatures were obtained from 2003 to 2012 (de Rosnay et al., 2006). Remote sensing and in situ soil measurements are available over fallow and bare-soil plots.

A number of studies have been conducted in recent years to investigate the relevance of using variational and Kalman filtering to analyze soil moisture. In 2000, the German Weather Service (Deutscher Wetterdienst) implemented a Simplified Extended Kalman Filter (SEKF) soil moisture analysis using screen-level parameter information Hess (2001). Four years later, Balsamo et al. (2004) introduced an online simplified 2-D-VAR method instead of a SEKF to retrieve soil moisture. More recently, Météo-France developed an offline SEKF to analyze soil moisture in the SURface EXternalized (SURFEX) system for research applications (Mahfouf et al., 2009). For the German and French models, the same approach of explicitly computing Jacobians in finite differences based on perturbed simulations is used. In 2010, a new LDAS based on a SEKF was implemented at the European Center for Medium-Range Weather Forecasts (ECMWF) in the global operational Integrated Forecasting System (IFS) (de Rosnay et al., 2012).

In the present work, a SEKF is used to assimilate in situ observations, gathered at SMOSREX over bare soil, into the Interactions between Surface, Biosphere, and Atmosphere (ISBA) LSM. Only the surface soil moisture (SSM) measured from the surface to 6 cm depth at 06:00 Local Standard Time (LST) is assimilated in the LDAS, if the observation is available. This experimental setup is used to represent the daily assimilation of remote sensing data at dawn. For example, SMOS has an ascending equator crossing time at 06:00 LST. Two versions of ISBA are used: the original force

restore scheme (Noilhan and Mahfouf, 1996) and a more complex diffusion scheme using Richards equations (Decharme et al., 2011). Hereafter, the two ISBA versions are referred to as ISBA-2L and ISBA-DF, respectively. The implementation of SEKF within ISBA-2L has been investigated by several authors such as Draper et al. (2011),
5 Barbu et al. (2011) and Albergel et al. (2010). In these studies, a two- or three-soil-layer configuration was used. Unlike ISBA-2L, ISBA-DF allows a fine discretization of the soil to be used (11 soil layers are considered). In this study, a first attempt is made to use the ISBA-DF in a data assimilation experiment. This work focuses on a bare soil site in order to isolate the thermal and water transfers in the soil without any interference
10 from processes related to the vegetation, such as transpiration. Decharme et al. (2011) had already studied differences between ISBA-2L and ISBA-DF using SMOSREX data over the fallow site. The behavior of these two LSMs over bare soil has not yet been compared. The period under investigation extends over three contrasted years from 2003 to 2005, including the 2003 drought. In addition, the role of bias correction in the
15 assimilation is discussed regarding the mass balance in the root zone. Despite the lack of a root-zone in the bare soil, this term will be used below to represent the total active soil depth.

The main objectives of this study are (1) to compare the soil moisture simulations from ISBA-2L and ISBA-DF over the bare soil, (2) to evaluate the role of SSM assim-
20 ilation for these two LSMs and (3) to investigate different configurations of ISBA-DF LDAS in four sensitivity cases. The SMOSREX data, IBSA-2L and ISBA-DF LSM and the SEKF algorithm are presented in Sect. 2. Assimilation results and sensitivity studies are presented in Sect. 3 and discussed in Sect. 4. Section 5 summarizes the main conclusions of the study.

2 Material and methods

2.1 The SMOSREX site and the soil moisture time series

The SMOSREX long-term experiment (2001–2012) was aimed at improving the modeling of land surface processes in the context of the SMOS mission (de Rosnay, 2006). The SMOSREX site is located in southwestern France (43°23′ N, 1°17′ E, at 188 m altitude) and is divided into two parts: a bare soil plot and a fallow plot. Soil moisture was measured at depths of 0–0.06, 0.10, 0.20, 0.30, 0.40, 0.50, 0.60, 0.70, 0.80 and 0.90 m every half hour. Soil probes were calibrated from gravimetric measurements (Schmugge et al., 1980). A weather station measured precipitation, 2 m air temperature and air humidity, 10 m wind speed, atmospheric pressure, and incoming solar and atmospheric radiation every 30 min. An L-band radiometer called LEWIS (Lemaître et al., 2004) measuring brightness temperature at two polarizations and five different angles is also present at the SMOSREX site. In this study, we focus on the bare soil plot. The percentage of sand and clay observed from 0.1 m to 0.90 m depth for bare soil on the SMOSREX is displayed in Fig. 1a.

Only the years 2003, 2004 and 2005 were considered because, for the bare soil plot, the soil moisture data at depths ranging from 0.20 m to 0.90 m are missing from 2006 onwards. The surface soil moisture (SSM) measurements, i.e. from the surface to 6 cm, were used for assimilation and measurements from 10 cm to 95 cm were used for validation purposes. In order to avoid frozen soil conditions, SSM observations made when the surface temperature was below a threshold of 4 °C were discarded.

2.2 Land surface models

The ISBA land surface model (Noilhan and Planton, 1989; Noilhan and Mahfouf, 1996) describes the surface processes in weather and climate applications. This model shows the evolution of land surface state variables (surface and soil temperatures, surface and root-zone soil moisture content) and the exchanges of heat and water

between the low level atmosphere, the vegetation and the soil. In this study, the SUR-FEX (SURFace EXternalisée) modeling platform (Masson et al., 2012) version 7.2 containing the ISBA LSM was used. SURFEX is designed for research and operational applications and includes several options of ISBA. In this study, SURFEX is forced by local atmospheric observations and run without feedback between the surface and the atmosphere (i.e. SURFEX is used offline). Moreover, to match measurement levels, the total soil depth was set to 0.95 m. The two options of the ISBA LSM (ISBA-2L and ISBA-DF) used in this study are summarized below.

2.2.1 ISBA-2L

The ISBA-2L version of SURFEX is based on the force restore approach, according to Deardorff (1977). This LSM is used in the operational NWP models at Météo-France. The soil is composed of two layers, the first layer being represented by a skin soil top layer 1 cm thick and the second by a bulk reservoir. The first layer is used to compute the SSM and soil evaporation while the second layer is used to compute the total soil moisture and contributes to the evapotranspiration (Boone et al., 1999). Mahfouf and Noilhan (1996) introduced a representation of gravitational drainage. In the force restore equations, the soil moisture dynamics depends on several thresholds (saturation (w_{sat}), wilting point (w_{wilt}), and field capacity (w_{fc})). These parameters are related to the soil textural properties (Mahfouf and Noilhan, 1996). In this work, w_{fc} was set to 0.30 m^3 m^{-3} in accordance with the measurements. w_{sat} and w_{wilt} were computed by ISBA-2L with respect to the sand and clay fractions and were equal to 0.45 m^3 m^{-3} and 0.17 m^3 m^{-3}, respectively. The modeled surface soil moisture and root zone soil moisture are referred to hereafter as w_1 and w_{tot} respectively.

2.2.2 ISBA-DF

The ISBA-DF LSM is a new ISBA version including a soil multi-layer diffusion scheme (Decharme et al., 2011), which explicitly solves mass and heat-diffusive equations. The

ISBA-DF soil hydrology uses the "mixed" form of the Richards equation to describe the water mass transfer within the soil via Darcy's law. Moisture and temperature profiles can be computed according to the vertical soil texture properties. Computations are performed using the SMOSREX soil texture displayed in Fig. 1a. In ISBA-DF, unlike in ISBA-2L, the soil moisture dynamics does not depend on the specification of a volumetric field capacity. In this study, 11 soil layers were considered, corresponding to the locations of observation instruments at the SMOSREX site. Figure 1b shows the soil discretization used in the ISBA-DF LSM and the placement of each probe. The node of each ISBA-DF soil layer corresponds to the depth of each probe: 0.10, 0.20, 0.30, 0.40, 0.50, 0.60, 0.70, 0.80 and 0.90 m. Close to the surface, two layers were considered: 0–0.01 m and 0.01–0.05 m. Hereafter, soil moisture in the n-th layer is denoted by w_n and the total soil water w_{tot} is the weighted average of w_n.

2.3 The simplified extended Kalman filter

In this section, the classical notations of data assimilation proposed by Ide et al. (1997) are used. The equation for the i-th model state forecast and update at time step t_i is:

$$\boldsymbol{x}^{b}(t_i) = \mathcal{M}_{i-1}\left[\boldsymbol{x}^{a}(t_{i-1})\right] \tag{1}$$

The equation for the i-th state analysis, occurring at time t_i is:

$$\boldsymbol{x}^{a}(t_i) = \boldsymbol{x}^{b}(t_i) + \mathbf{K}_i\left(\boldsymbol{y}^{o}_i - \mathcal{H}_i[\boldsymbol{x}^{b}(t_i)]\right) \tag{2}$$

where $\boldsymbol{x}$ indicates the model state and $\boldsymbol{y}^{o}$ is the observation vector. The superscripts a, b and o indicate the analysis, the background and the observations, respectively. Analysis increments are the difference between the analysis and the background. $\mathcal{M}$ is the nonlinear forecast model and $\mathcal{H}$ is the nonlinear observation operator. Both in ISBA-2L and ISBA-DF, the observation vector is $\boldsymbol{y}^{o} = (SSM)$. The model state vector is different following the LSM used:

$$x_{\text{ISBA-2L}} = [w_1, w_{\text{tot}}] \tag{3}$$

$$x_{\text{ISBA-DF}} = [w_1, w_2, w_3, w_4, w_5, w_6, w_7, w_8, w_9, w_{10}, w_{11}] \tag{4}$$

The observations occurred 24 h after the analysis time and $\mathcal{H}$ includes a 24 h integration of the forecast model (Draper et al., 2011). The available observations are assimilated at 06:00 LST. The Kalman gain is given by:

$$\mathbf{K}_i = \mathbf{B}_i \mathbf{H}_i^{\mathsf{T}} \left(\mathbf{H}_i \mathbf{B}_i \mathbf{H}_i^{\mathsf{T}} + \mathbf{R}_i \right)^{-1} \tag{5}$$

where the Jacobian matrix $\mathbf{H}$ is the linearization of $\mathcal{H}$ and $\mathbf{H}^{\mathsf{T}}$ its transpose. $\mathbf{H}$ is obtained using a finite difference approach, by individually perturbing each component x_j of the initial model state x at time t_0 by a small amount δx_j. The Jacobian is expressed as the difference of the prognostic states between perturbed and reference runs at the end of the assimilation interval at time t_i, divided by the initial perturbation:

$$\mathbf{H} = \frac{\mathcal{H}(x + \delta x_j) - \mathcal{H}(x)}{\delta x_j} \tag{6}$$

For all the experiments, the perturbation size is set to $0.001\,\text{m}^3\,\text{m}^{-3}$. Mahfouf et al. (2009) have showed that these very small perturbations lead to good approximations of the linear behavior of the observation operator. The Jacobian values are computed with a daily time step ($t_i - t_0 = 24\,\text{h}$). The examination of the Jacobian matrices is important for understanding the data assimilation performance. $\mathbf{B}$ and $\mathbf{R}$ are the covariance matrices of the background and observations errors, respectively. The SEKF does not cause $\mathbf{B}$ to evolve through a forecast cycle, unlike the traditional EKF. Draper et al. (2009) found that, for assimilating near-surface soil moisture into ISBA LSM, the analyzed soil moisture generated by the EKF and the SEKF were not substantially different. This result is explained by the fact that the increase in the background error during each

forward propagation step is balanced by the decrease in the error during the analysis step and the difficulties of specifying the **Q** matrix (model error). Moreover, Sabater et al. (2007) suggested that, at the SMOSREX location, a fixed background error was more accurate and stable than an evolving background error.

The performance of an analysis scheme depends on the use of appropriate statistics for background and observation errors. For all the experiments, the observation standard deviation error for SSM was set to $0.02\,\mathrm{m^3\,m^{-3}}$. This error is consistent with that chosen by Sabater et al. (2007) at the SMOSREX site.

In the ISBA-2L assimilation experiment, **B** was a diagonal matrix with the standard deviation errors σ_{w_1} and $\sigma_{w_{\mathrm{tot}}}$ set to $0.02\,\mathrm{m^3\,m^{-3}}$ and $0.005\,\mathrm{m^3\,m^{-3}}$, respectively. The ratio between σ_{w_1} and $\sigma_{w_{\mathrm{tot}}}$ was equal to one used by Albergel et al. (2010).

Concerning ISBA-DF, the experiments were carried out using a **B** diagonal matrix with the same background standard deviation error σ_{w_n} along the diagonal ($0.015\,\mathrm{m^3\,m^{-3}}$) except that σ_{w_1} was set to $0.02\,\mathrm{m^3\,m^{-3}}$. The values were adjusted to obtain results not too different from those with ISBA-2L results on average. This representation of the **B** matrix considers that the soil layer errors are not correlated. However, in ISBA-DF LSM, the layers are linked through diffusive equations. Thus, errors in a given layer should affect the others. Several experiments described below used a tri-diagonal **B**$_{\mathrm{tri\text{-}diag}}$ matrix in order to propagated error through the adjacent layers. The **B**$_{\mathrm{tri\text{-}diag}}$ matrix is expressed as:

$$
\mathbf{B}_{\mathrm{tri\text{-}diag}} = \begin{pmatrix}
\sigma_{w_1}^2 & \alpha\,\sigma_{w_1}\sigma_{w_2} & 0 & 0 & 0 \\
\alpha\,\sigma_{w_2}\sigma_{w_1} & \ddots & \ddots & \ddots & 0 \\
0 & \ddots & \sigma_{w_n}^2 & \ddots & 0 \\
0 & \ddots & \ddots & \ddots & \alpha\,\sigma_{w_{10}}\sigma_{w_{11}} \\
0 & 0 & 0 & \alpha\,\sigma_{w_{11}}\sigma_{w_{10}} & \sigma_{w_{11}}^2
\end{pmatrix}
$$

where the correlation term α is empirically set to 0.5.

Numerous studies (Reichle and Koster, 2004; Pellarin et al., 2006; Rüdiger et al., 2007) have shown the necessity to rescale data before assimilating in situ or satellite-derived soil moisture in order to reduce systematic biases between the model and observations. In this study the CDF-matching technique proposed by Reichle and Koster

5 (2004) is used for all the experiments and described in Sect. 3.1.

2.4 Design of the experiments

Six assimilation experiments were undertaken. The first two were performed using ISBA-2L and ISBA-DF. Hereafter, these experiments are referred to as 2L and DF-REF, respectively. The DF-REF configuration was chosen to be as close as possible

10 to the 2L configuration: the observations concerned the surface soil moisture (0–1 cm) equivalent and the **B** matrix was assumed diagonal for both experiments.

Then, starting from the DF-REF experiment, several modifications to the LDAS were considered. The experiment DF-H2 assimilated SSM into the second soil layer (1–5 cm) in order to better represent the SSM observations gathered between 0 and 6 cm.

15 Next, the experiment DF-B used a non-diagonal $\mathbf{B}_{\text{tri-diag}}$ matrix in order to account for the error correlations in adjacent soil layers as described in Sect. 2.3.

In addition, a bias correction technique performed before assimilation was included in the experiment DF-CDF. It allowed the impact of the temporal window chosen for data rescaling to be studied.

20 The last experiment, DF-NP, evaluated the benefit of assimilation in the case where ISBA-DF LSM was forced with a local forcing where the precipitation was set to zero. The role of the assimilation in LSM in compensating for a less accurate forcing will be shown below. In this experiment, the background state was not as reliable as in previous experiments since there was no precipitation. In this case, the background error

25 σ_{w_n} was increased by a factor of three (Albergel et al., 2010) and no bias correction was performed.

The characteristics of the experiments are listed in Table 1.

3 Results

3.1 CDF-matching technique

The histograms of the distributions of SSM observed at the SMOSREX site, and w_1 modeled by ISBA-2L and ISBA-DF are displayed in Fig. 2 for the 2003–2005 period. Note that SSM observations are measured between 0 and 6 cm depth. The SSM observation distribution has two modes. The first corresponds to observed values smaller than $0.17\,\mathrm{m^3\,m^{-3}}$ and represents 29 % of the population. The second mode concerns observed values greater than $0.17\,\mathrm{m^3\,m^{-3}}$ and represents 71 % of the population. The smallest SSM observation value is equal to $0.04\,\mathrm{m^3\,m^{-3}}$ whereas the largest value reaches $0.43\,\mathrm{m^3\,m^{-3}}$. The w_1 value modeled by ISBA-2L also presents two modes. A large fraction of the w_1 population (40 %) has values smaller than $0.18\,\mathrm{m^3\,m^{-3}}$, while 60 % of the population has values larger than this value. The smallest value of modeled w_1 is $0.04\,\mathrm{m^3\,m^{-3}}$. The largest value of w_1 computed by ISBA-2L is $0.37\,\mathrm{m^3\,m^{-3}}$. Concerning w_1 computed by ISBA-DF, the histogram of the distribution does not present two modes. The w_1 modeled with ISBA-DF has a lower dynamical range than the observations. The smallest value of w_1 modeled with ISBA-DF is $0.08\,\mathrm{m^3\,m^{-3}}$ and the largest is $0.35\,\mathrm{m^3\,m^{-3}}$. The values of w_2 computed by ISBA-DF have a weaker dynamic range than w_1 simulated by the same LSM. However, two modes are present. The first mode contains 54 % of the population for values lower than $0.24\,\mathrm{m^3\,m^{-3}}$ and the second mode represents 46 % of the population. The smallest value of the modeled w_2 is $0.014\,\mathrm{m^3\,m^{-3}}$, whereas the largest value reaches $0.36\,\mathrm{m^3\,m^{-3}}$.

The CDF matching proposed by Reichle and Koster (2004) was used in order to remove the bias between the observations and the modeled w_1. This bias correction scheme modifies the observations in order to make their statistical distribution closer to the one from the model. For this, a third-order polynomial fit is computed. Following Scipal et al. (2008), a large statistical sample needs to be considered to obtain a robust bias correction scheme.

Title Page

Abstract | Introduction

Conclusions | References

Tables | Figures

◀ | ▶

◀ | ▶

Back | Close

Full Screen / Esc

Printer-friendly Version

Interactive Discussion

The results of the CDF matching performed over this period for ISBA-2L and ISBA-DF are shown in Fig. 3. Observations rescaled with ISBA-2L and ISBA-DF do not exceed $0.34\,\mathrm{m^3\,m^{-3}}$ and $0.35\,\mathrm{m^3\,m^{-3}}$, respectively. The CDF matching plays an important role during wet and dry periods and thus reduces the seasonal dynamics by decreasing the SSM values in winter and increasing them in summer.

3.2 Assimilation experiments

3.2.1 2L experiment

Simulations performed without data assimilation are called "open-loop" simulations. Figure 4 shows the time series of w_1, w_{tot} and observations for the open-loop and the analysis simulations over the period 2003–2005. The annual w_1 is generally well reproduced by the model. In winter, the modeled w_1 are smaller than the observed values, except for the winter of 2005. The daily cycles and the rainfall responses are overestimated. The greatest differences between the open-loop and the analysis concern the winter and spring of 2003 and 2004. For 2003, the analysis values are higher than the open-loop values. The contrary is seen for 2004. No marked differences between open-loop and analysis simulations are observed for 2005. The temporal behavior of the w_{tot} is well represented except for the drought of 2003. During the 2003 heat wave, the open-loop shows larger soil moisture content values than were observed. The assimilation reduces the bias, allowing a better match with observations in this period. During the summers of 2004 and 2005, the assimilation tends to decrease the soil water content.

Several statistical scores (correlation coefficient r, Root Mean Square Error (RMSE), Standard Deviation Difference (SDD) and bias (model minus observations)) for the open-loop and the analysis w_1 simulations over the 3 yr period are summarized in Table 2. Over the 3 yr period, the w_1 analysis simulation is better correlated with the observations than the w_1 open-loop.

Title Page

Abstract | Introduction

Conclusions | References

Tables | Figures

◀ | ▶|

◀ | ▶

Back | Close

Full Screen / Esc

Printer-friendly Version

Interactive Discussion

The annual open-loop and analysis statistical scores for w_{tot} are given in Fig. 5. Assimilated SSM increases the correlation coefficient by 3 % and decreases the RMSE by 50 %.

The Jacobian terms $\frac{\partial w_1(t)}{\partial w_1(t_0)}$ and $\frac{\partial w_1(t)}{\partial w_{tot}(t_0)}$ in the first thin layer and in the bulk reservoir are illustrated in Fig. 6. Generally, the Jacobian terms have positive values. Zero and small negative values are also found, which represent 39 % and 15 % of the Jacobian terms for w_1 and w_{tot}, respectively. Over the 2003–2005 period, 14 % and 13 % of the Jacobian terms $\frac{\partial w_1(t)}{\partial w_1(t_0)}$ and $\frac{\partial w_1(t)}{\partial w_{tot}(t_0)}$, respectively, are strictly equal to zero. Null Jacobian values indicate that neither w_1 nor w_{tot} is sensitive to SSM assimilation. During wet periods, the Jacobian term for w_1 is equal or close to zero. For dry soils, SSM assimilation over a 24 h window does not modify the behavior of w_1. The mean values of the Jacobian term with respect to w_1 and w_{tot} are 0.15 and 0.51, respectively. Over a 24 h window, the impact of the SSM assimilation is higher in the bulk reservoir than in the first layer. This finding is consistent with previous studies, e.g. by Draper et al. (2009) and Mahfouf (2010).

3.2.2 DF-REF experiment

Figure 7 shows w_1 open-loop and analysis time series for DF-REF together with observations for 2003–2005. The statistical scores for w_1 open-loop and analysis simulations over the 3 yr period are listed in Table 2. The w_1 simulations performed with and without assimilation are better correlated with observations for ISBA-DF than ISBA-2L. Moreover, for both open-loop and analysis simulations obtained with ISBA-DF, the day-to-day variability is reduced compared with ISBA-2L simulations. This effect tends to decrease the RMSE by 20 % and 25 % respectively for the open-loop and analysis computed by ISBA-DF relative to those simulated by ISBA-2L.

The yearly w_{tot} open-loop and analysis time series are shown in Fig. 7. The statistical scores are displayed in Fig. 5. For both open-loop and analysis, the annual cycles are well represented by ISBA-DF and the statistical scores outperform those obtained by

ISBA-2L. On the one hand, unlike the ISBA-2L simulations, the open-loop reproduces the 2003 drought well and a perfect match with observations is noted during summer 2004. On the other hand, the open-loop root zone soil moisture is underestimated in 2005 in contrast to the ISBA-2L results. In 2003, the root zone soil moisture obtained after assimilation is closer to the observed values than that in the open-loop results. During the spring of 2004 and 2005 and the summer of 2004, the SSM observations are drier than the model counterpart values, even after CDF matching. This results in a large decrease in surface soil moisture content after assimilation.

Figure 8 shows the w_1 open-loop and analysis for four different layers i: layer 2 (1–5 cm), layer 4 (15–25 cm), layer 6 (35–45 cm) and layer 8 (35–45 cm). For w_2 and w_4, the open-loop and analysis represent the annual cycle well. After assimilation, w_2 and w_4 are better correlated with observations and the bias is smaller for the w_2 analysis than for the open-loop by 0.004 m^3 m^{-3}. Concerning w_6 and w_8, the annual cycle is overestimated compared to the observations. For the whole year 2005, open-loop and analysis w_6 and w_8 are found to be very dry. The same behavior is observed during the summer of 2004. From layer 7 (−45 cm), assimilation decreases the statistical scores slightly.

The Jacobian, the Kalman gain **K** and analysis increments permit the performance of the data assimilation to be evaluated. Figure 9 shows the time evolution of the Jacobian terms $\frac{\partial w_1(t)}{\partial w_n(t_0)}$, the Kalman gain and the increments for each layer n.

The largest Jacobian values are obtained for the layers 2, 3 and 4 (i.e. depths of 1–25 cm). The mean Jacobian values for these layers are: 0.19, 0.28 and 0.15, respectively. For deeper layers, the mean Jacobian value is lower than 0.10. The assimilation does not play an important role in the first layer or in layers 5 to 11. During wet periods, the Jacobian in the full soil column is small but not strictly equal to zero. The Kalman gain behaves similarly. During dry periods, the information provided at the surface does not penetrate very deeply into the soil due to low values of hydraulic conductivity. The maximum values of the Jacobian and the Kalman gain are observed during summers for the second layer, while the maximum values in other layers are noted in autumn

and spring. In the deep layers (layers from 5 to 11), maximum Jacobian and Kalman gain values are reached in winter due to larger values of hydraulic conductivity. From the Kalman gain value, and in contrast to 2L, the LDAS does not perform corrections over the total soil column but in individual layers that vary with the seasonal cycle. Note that the sum of the Jacobian values in each layer is, on average, close to the average of the sum of the Jacobian in the two layers used in 2L.

The analysis increments allow the impact of the data assimilation on the water mass balance to be investigated. During the summers of 2003 and 2005, only the ten first centimeters of soil are sensitive to the assimilation. For the whole year 2004, 73 % of the increments are negative. As a result, the assimilation tends to remove water in most instances. For example, from January to May 2004, the increments are essentially negative. In layers 1 to 5 (from the surface to -35 cm), 87 % of the increments are different from zero. For deeper layers, the fraction of non-zero increments decreases, to reach 35 % for the last layer.

3.3 Sensitivity studies in ISBA-DF

In this section, results of the four experiments presented in Table 1 are examined.

3.3.1 Second soil layer assimilation

The SSM observations are measured between the surface and 6 cm depth. In contrast to the previous experiments, DF-H2 was carried out in order to assimilate SSM in the second layer of ISBA-DF. The depth of this layer (1–5 cm) is closer to the observation depth. CDF matching is performed between w_2 and the observations over the 3 yr period to remove systematic biases.

Statistical scores of w_1 analysis for the 3 yr period are displayed in Table 2. Over this time, the assimilation in the second layer tends to decrease the RMSE of the w_1 with respect to the DF-REF. However, the correlation coefficient of w_1 computed by DF-H2 is weaker than those simulated by DF-REF.

Yearly statistical scores of w_{tot} are shown in Fig. 5. The RMSE of root zone soil moisture is slightly smaller for the analysis using DF-H2 than DF-REF. Over the full period, assimilating SSM in the second layer decreases the bias by 84 % compared with DF-REF. The non-zero increments increase by 3 % for deeper layers (−35 cm to −95 cm) with respect to the reference experiment. For layers 1 to 5, no significant impact is observed.

Figure 10 shows the time evolution of w_2 open-loop and the Jacobian term $\frac{\partial w_2(t)}{\partial w_2(t_0)}$ for DF-H2 and $\frac{\partial w_1(t)}{\partial w_2(t_0)}$ for DF-REF. For both experiments, the Jacobian is larger during dry periods than during wet periods. In the wet season (winter) and for rainy events, the Jacobians are very low, indicating that initial soil moisture perturbations are lost during the 24 h model integration. In such situations, the soil moisture in the first two layers is therefore mostly driven by the atmospheric forcing. As seen in Fig. 10, the Jacobian $\frac{\partial w_1(t)}{\partial w_2(t_0)}$ is more sensitive to rainfall events when the SSM is assimilated in the first layer than in the second layer. Since the second layer is less impacted by the atmospheric forcing than the first layer, assimilating the observations in the second layer overcomes the effect of rainfall events and allows more information to be extracted.

3.3.2 The choice of the B matrix

Experiment DF-B was undertaken with the $\mathbf{B}_{tri-diag}$ matrix in order to propagate model error in adjacent layers. The statistical scores of w_1 analysis over the 3 yr period are displayed in Table 2. Compared with DF-REF, a slight increase in the correlation coefficient and a decrease in RMSE are observed. The SDD falls by 42 % relative to the reference experiment. Yearly statistical scores of w_{tot} analysis are shown in Fig. 5. Statistical scores of DF-REF and DF-B are close.

The $\mathbf{B}_{tri-diag}$ matrix has an important impact on the Kalman gain. Figure 11 shows the difference between the Kalman gain computed by the assimilation in DF-B and DF-REF. Adding correlation terms to the B matrix increases the Kalman gain values from 1 cm to 35 cm depth and for deeper layers during wet periods. For these layers during

dry periods, the Kalman gain is strictly zero in DF-REF. Over the 3 yr period, the mean Kalman gain values increase by 27 % in the DF-B relative to DF-REF.

An assimilation experiment with a five-band **B** matrix was also performed to increase vertical correlations (not shown). The statistical scores of w_{tot} analysis over the 3 yr period were close to those obtained with DF-B. However, the average Kalman gain values increased by 21 % with respect to DF-B.

3.3.3 Impact of the CDF-matching on the water mass balance

In this section, the impact of CDF matching on the water mass balance is investigated. CDF matching year per year is computed in the experiment DF-CDF but not in DF-REF. A third-order polynomial fit is computed for each individual year. Figure 12 shows the CDF for the SSM observations, modeled w_1, and SSM rescaled observations for 2003, 2004 and 2005. Generally, CDF matching reduces the dynamical range of the observations. Concerning 2003, only the largest values are reduced. For 2004, dry SSM observations (below $0.30\,\mathrm{m}^3\,\mathrm{m}^{-3}$) are increased to match to the modeled w_1. The same feature is seen for 2005: the observation values are augmented until $0.27\,\mathrm{m}^3\,\mathrm{m}^{-3}$ and reduced for dry values. CDF matching performed over the 3 yr period is also shown in Fig. 12. The SSM CDF in 2003 and 2004 do not have the same features as the CDF performed over the three years. Therefore, rescaled SSM in 2003 and 2004 will be different from SSM rescaled with the CDF matching performed over the 3 yr period.

The w_1 analysis statistical scores performed with DF-CDF are displayed in Table 2. The correlation of w_1 increases by 14 % with respect to the open-loop. Compared with DF-REF w_1 analysis, a slight increase (3 %) of the correlation coefficient is noted. The RMSE decreases by 47 % with respect to the open-loop and by 10 % relative to w_1 analysis computed with DF-REF.

Over the 3 yr period, the correlation coefficient, RMSE, SDD and bias values of the w_{tot} analysis are 0.90, $0.052\,\mathrm{m}^3\,\mathrm{m}^{-3}$, $0.052\,\mathrm{m}^3\,\mathrm{m}^{-3}$ and $-0.006\,\mathrm{m}^3\,\mathrm{m}^{-3}$, respectively. A slight increase of the statistical scores is noted with respect to DF-REF (Fig. 5).

The main difference between DF-REF and DF-CDF is obtained during 2004 where the RMSE of w_{tot} decreases by 13 %.

The increments provided by the assimilation scheme using CDF matching year per year are shown in Fig. 13. For 2005, no significant differences are observed. However, for 2003 and 2004, differences between increments obtained with DF-REF and DF-CDF are clear. Using an annual CDF allows the water mass balance to be conserved in the root zone. For example, in 2003, water from the root zone is removed between January and April in DF-CDF whereas water is still added during the same period in DF-REF. The same feature is observed during the full year of 2004: water in the soil is systematically removed in several consecutive months in DF-REF but in DF-CDF, significant water amounts are added. Moreover, using annual CDF-matching improves the simulation of the root zone soil moisture for the years when the SSM distribution is very different from the average SSM distribution.

3.3.4 Forcing without precipitation

Removing precipitation from the forcing permits the benefit of the SSM assimilation to be evaluated when the forcing is not accurate. No CDF-matching technique is used over the assimilated SSM. The statistical scores of w_1 analysis are shown in Table 2. The statistical scores are improved compared to those of DF-REF. For example, the correlation coefficient is increased by 9 % and the RMSE is decreased by 43 % with respect to the reference experiment.

The statistical scores computed year per year for w_{tot} analysis are displayed in Fig. 5. Despite the lack of precipitation in the forcing, statistics are close to the DF-REF open-loop simulation. Good statistical results are due to the increase in the background error in DF-NP with respect to DF-REF.

Time series of the root zone soil moisture with and without assimilation for the experiment DF-NP are shown in Fig. 14. Without precipitation, w_{tot} simulated by the open-loop goes down while the analysis maintains the annual cycle.

From an operational point of view, the SSM assimilation in ISBA-DF LSM allows forcing uncertainties to be overcome, even though the current test was performed in extreme conditions.

4 Discussion

In the ISBA-2L LSM, the hydrologic soil parameter w_{fc} has to be calibrated for good agreement between computed and observed soil moisture at the SMOSREX bare soil site. Moreover, this LSM is used for operational NWP predictions at Météo-France and has been widely studied. For ISBA-DF LSM, no tuning of hydrological parameters is needed. This makes the ISBA-DF more flexible for regional or global applications. At the moment, unlike ISBA-2L, ISBA-DF is a new LSM that is starting to be tested and is used only for research applications. Soil moisture computed by ISBA-DF is better correlated with observations than that simulated by ISBA-2L. This result is consistent with the finding of Decharme et al. (2011) on the fallow part of the SMOSREX site. Over the 3 yr period, an improvement in terms of statistical scores is found for both w_1 and w_{tot} when simulated by ISBA-DF rather than ISBA-2L.

The SSM assimilation improves the modeling of w_1 and w_{tot} for the two LSMs. In 2L, corrections introduced by the assimilation affect the whole root zone. This feature is not realistic, particularly for a bare soil surface (Draper et al., 2009). The propagation of SSM information to deeper soil layers is consistent with the water transfer physics in ISBA-DF. The assimilation does not have the same impact on the soil moisture content at different soil depths. For example, during dry periods, corrections introduced by the LDAS are located at depths between 1 and 25 cm. Weaker corrections were found to impact the total soil column during wet periods.

As seen in the previous sections, for all the experiments carried out with ISBA-DF LSM, the assimilation of SSM has little impact in the first layer (0–1 cm). For example, the mean Jacobian $\frac{\partial w_1(t)}{\partial w_1(t_0)}$ for DF-REF is equal to 0.034 in the first layer. In contrast, the

mean Jacobians $\frac{\partial w_1(t)}{\partial w_2(t_0)}$, $\frac{\partial w_1(t)}{\partial w_3(t_0)}$ and $\frac{\partial w_1(t)}{\partial w_4(t_0)}$ are larger than 0.1. This result is surprising because one would expect a strong impact of the assimilation in the first layer as in 2L. Due to the small size of the w_1 reservoir (1 cm), the dynamics of the first layer is driven by the atmospheric forcing. Moreover, in the experimental setup, the length of the assimilation window is 24 h. Over this time period, the impact of the initial conditions is reduced by the atmospheric forcing. Similar results were found with DF-H2 with small values of the Jacobians in the first layer. This result is in agreement with a recent study by Medina et al. (2012) also showing a weak impact of the Kalman filter in the first layer.

Accounting for vertical correlations in the background error covariance matrix, $\mathbf{B}_{\text{tri-diag}}$, of the SEKF scheme tends to decrease the RMSE of w_1. Despite an increase in Jacobian and Kalman gain values, no significant improvement to the analysis of w_{tot} has been noticed. In future studies, it would be desirable to work with an EKF scheme instead of an SEKF to benefit from the evolution of the $\mathbf{B}$ matrix. An evolutive $\mathbf{B}$ matrix would take the vertical correlation errors into account better. However, more research needs to be done to improve the specification of model errors. Assimilating SSM in the second layer appears to be more physically meaningful.

After assimilation of SSM in the second layer, the bias of w_{tot} analysis is small. Over the 3 yr period, DF-H2 appears to be the best experiment in terms of RMSE and bias.

Numerous studies have proposed to rescale the observations before assimilating them into an LSM. Several authors have performed CDF matching over the entire period of interest (Reichle and Koster, 2004), whereas others have used seasonal-based CDF matching (Barbu et al., 2013; Draper et al., 2009). As shown in Sect. 3, using CDF matching year per year constrains the mass balance better, essentially for 2004. In southwestern France, the yearly SSM distribution is very different from one year to another and global CDF matching erases the interseasonal variability of the model dynamics. Yearly CDF matching is advocated for reanalysis systems even though it is not suitable for real time monitoring or forecasting.

Other assimilation studies at the SMOSREX site were performed in order to improve the root-zone soil moisture (Sabater et al., 2007; Albergel et al., 2010). Unlike this study, they were focused on the fallow part of the SMOSREX site. Over the bare soil, the root-zone dynamics and the response to rainfall events are larger than over the fallow area. In this study, similar results to those of Sabater et al. (2007) and Albergel et al. (2010) were found using the 2L model.

5 Conclusions

This study investigated the assimilation performances of two versions of the land surface model ISBA: (1) ISBA-2L with a soil composed of two layers and (2) ISBA-DF with a soil divided into 11 layers. This work was carried out on the SMOSREX bare-soil site during the period 2003–2005. This was a first attempt to explore the potential of assimilating SSM using an SEKF over France with ISBA-DF. Regarding open-loop simulations, w_1 and w_{tot} simulated by ISBA-DF outperformed those computed by ISBA-2L with an ad-hoc adjustment of w_{fc}.

The largest impact of the SSM assimilation with ISBA-DF concerns the first 45 cm of soil. For dry periods, the SSM assimilation plays an important role from the surface to 25 cm whereas, during wet periods, weak corrections are applied for the entire soil column. These seasonal variations cannot be represented with a single bulk layer in the root zone. For the first time, the evolution of the Jacobian terms, the Kalman gain and the increments with depth have been examined.

The best improvement of w_{tot} analysis was obtained by assimilating SSM in the second layer. This result shows the interest of working with a multi-layer LSM. Assimilating the SSM in the second layer and adding vertical correlation errors are recommended for future research. Yearly CDF matching leads to a better conservation of the water mass balance in the root zone and is encouraged for data re-analyses.

This work shows the potential to improve the soil moisture in the deep layers by assimilating SSM in ISBA-DF. This study will be extended to the whole of France by

assimilating satellite-derived SSM such as ASCAT and SMOS. In addition, the assimilation of brightness temperature from the L band radiometer LEWIS in ISBA-DF would be interesting. The impact on the other terms of water balance (surface evaporation and runoff) was not examined because of the lack of suitable observations over the bare soil plot of SMOSREX.

References

Albergel, C., Calvet, J.-C., Mahfouf, J.-F., Rüdiger, C., Barbu, A. L., Lafont, S., Roujean, J.-L., Walker, J. P., Crapeau, M., and Wigneron, J.-P.: Monitoring of water and carbon fluxes using a land data assimilation system: a case study for southwestern France, Hydrol. Earth Syst. Sci., 14, 1109–1124, doi:10.5194/hess-14-1109-2010, 2010. 9649, 9654, 9655, 9666

Balsamo, G., Bouyssel, F., and Noilhan, J.: A simplified bi-dimensional variational analysis of soil moisture from screen-level observations in a mesoscale numerical weather-prediction model, Q. J. Roy. Meteorol. Soc., 130, 895–915, 2004. 9648

Balsamo, G., Mahfouf, J., Bélair, S., and Deblonde, G.: A land data assimilation system for soil moisture and temperature: an information content study, J. Hydrometeorol., 8, 1225–1242, 2007. 9647

Barbu, A. L., Calvet, J.-C., Mahfouf, J.-F., Albergel, C., and Lafont, S.: Assimilation of Soil Wetness Index and Leaf Area Index into the ISBA-A-gs land surface model: grassland case study, Biogeosciences, 8, 1971–1986, doi:10.5194/bg-8-1971-2011, 2011. 9649

Barbu, A. L., Calvet, J.-C., Mahfouf, J.-F., and Lafont, S.: Assimilation of Soil Wetness Index and Leaf Area Index into ISBA-A-gs land surface model over France, Hydrol. Earth Syst. Sci., submitted, 2013. 9665

Bartalis, Z., Wagner, W., Naeimi, V., Hasenauer, S., Scipal, K., Bonekamp, H., Figa, J., and Anderson, C.: Initial soil moisture retrievals from the METOP-A Advanced Scatterometer (ASCAT), Geophys. Res. Lett., 34, L20401, doi:10.1029/2007GL031088, 2007. 9647

Boone, A., Calvet, J.-C., and Noilhan, J.: Inclusion of a third soil layer in a land surface scheme using the forcerestore method, J. Clim. Appl. Meteorol., 38, 1611–1630, 1999. 9651

Crow, W. and Wood, E.: The assimilation of remotely sensed soil brightness temperature imagery into a land surface model using ensemble Kalman filtering: a case study based on ESTAR measurements during SGP97, Adv. Water Resour., 26, 137–149, 2003. 9647

Deardorff, J.: A parameterization of ground-surface moisture content for use in atmospheric prediction models, J. Appl. Meteorol., 16, 1182–1185, 1977. 9651

Decharme, B., Boone, A., Delire, C., and Noilhan, J.: Local evaluation of the Interaction between soil biosphere atmosphere soil multilayer diffusion scheme using four pedotransfer functions, J. Geophys. Res., 116, D20126, doi:10.1029/2011JD016002, 2011. 9649, 9651, 9664

de Rosnay, P., Calvet, J.-C., Kerr, Y., Wigneron, J.-P., Lematre, F., Escorihuela, M. J., Sabater, J. M., Saleh, K., Barri, J., Bouhours, G., Coret, L., Cherel, G., Dedieu, G., Durbe, R., Fritz, N. E. D., Froissard, F., Hoedjes, J., Kruszewski, A., Lavenu, F., Suquia, D., and Waldteufel, P.: SMOSREX: a long term field campaign experiment for soil moisture and land surface processes remote sensing, Remote Sens. Environ., 102, 377–389, doi:10.1016/j.rse.2006.02.021, 2006. 9648

de Rosnay, P., Drusch, M., Vasiljevic, D., Balsamo, G., Albergel, C., and Isaksen, L.: A simplified Extended Kalman Filter for the global operational soil moisture analysis at ECMWF, Q. J. Roy. Meteorol. Soc., online first, doi:10.1002/qj.2023, 2012. 9648

Draper, C. S., Mahfouf, J.-F., and Walker, J. P.: An EKF assimilation of AMSR-E soil moisture into the ISBA land surface scheme, J. Geophys. Res., 114, D20104, doi:10.1029/2008JD011650, 2009. 9653, 9658, 9664, 9665

Title Page

Abstract | Introduction

Conclusions | References

Tables | Figures

|◀ | ▶|

◀ | ▶

Back | Close

Full Screen / Esc

Printer-friendly Version

Interactive Discussion

Draper, C., Mahfouf, J.-F., Calvet, J.-C., Martin, E., and Wagner, W.: Assimilation of ASCAT near-surface soil moisture into the SIM hydrological model over France, Hydrol. Earth Syst. Sci., 15, 3829–3841, doi:10.5194/hess-15-3829-2011, 2011. 9649, 9653

Entekhabi, D., Nakamura, H., and Njoku, E.: Solving the inverse problem for soil moisture and temperature profiles by sequential assimilation of multifrequency remotely sensed observations, IEEE T. Geosci. Remote, 32, 438–448, 1994. 9647

Entekhabi, D., Asrar, G., Betts, A., Beven, K., Bras, R., Duffy, C., Dunne, T., Koster, R., Lettenmaier, D., McLaughlin, D., Shuttleworth, W. J., van Genuchten, M. T., Wei, M.-Y., and Wood, E. F.: An agenda for land surface hydrology research and a call for the second international hydrological decade, B. Am. Meteorol. Soc., 80, 2043–2058, 1999. 9647

Entekhabi, D., Njoku, E., Houser, P., Spencer, M., Doiron, T., Kim, Y., Smith, J., Girard, R., Belair, S., Crow, W., Jackson, T. J., Kerr, Y. H., Kimball, J. S., Koster, R., McDonald, K. C., O'Neill, P. E., Pultz, T., Running, S. W., Shi, J., Wood, E., and Van Zyl, J.: The hydrosphere state (Hydros) satellite mission: an earth system pathfinder for global mapping of soil moisture and land freeze/thaw, IEEE T. Geosci. Remote, 42, 2184–2195, 2004. 9647

Hess, R.: Assimilation of screen-level observations by variational soil moisture analysis, Meteorol. Atmos. Phys., 77, 145–154, 2001. 9648

Houser, P. R., Shuttleworth, W. J., Famiglietti, J. S., Gupta, H. V., Syed, K. H., and Goodrich, D. C.: Integration of soil moisture remote sensing and hydrologic modeling using data assimilation, Water Resour. Res., 34, 3405–3420, 1998. 9647

Ide, J., Courtier, P., Ghil, M., and Lorenc, A.: Unified notation for data assimilation: operational, sequential and variational, J. Meteorol. Soc. Jpn., 75, 181–189, 1997. 9652

Kerr, Y., Waldteufel, P., Wigneron, J., Martinuzzi, J., Font, J., and Berger, M.: Soil moisture retrieval from space: the Soil Moisture and Ocean Salinity (SMOS) mission, IEEE T. Geosci. Remote, 39, 1729–1735, 2001. 9647

Koster, R. and Suarez, M.: Relative contributions of land and ocean processes to recipitation variability, J. Geophys. Res., 100, 13775–13790, doi:10.1029/95JD00176, 1995. 9647

Lemaître, F., Poussière, J.-C., Kerr, Y. H., Déjus, M., Durbe, R., de Rosnay, P., and Calvet, J.-C.: Design and test of the ground-based L-band radiometer for estimating water in soils (LEWIS), IEEE T. Geosci. Remote, 42, 1666–1676, 2004. 9650

Mahfouf, J.-F.: Assimilation of satellite-derived soil moisture from ASCAT in a limited-area NWP model, Q. J. Roy. Meteor. Soc., 136, 784–798, 2010. 9658

Design and evaluation at local scale

M. Parrens et al.

Title Page

Abstract	Introduction
Conclusions	References
Tables	Figures

|◀ | ▶|

◀ | ▶

Back | Close

Full Screen / Esc

Printer-friendly Version

Interactive Discussion

Mahfouf, J. F. and Noilhan, J.: Inclusion of gravitational drainage in a land surface scheme based on the force-restore method, J. Appl. Meteorol., 35, 987–992, 1996. 9651

Mahfouf, J.-F., Bergaoui, K., Draper, C., Bouyssel, F., Taillefer, F., and Taseva, L.: A comparison of two off-line soil analysis schemes for assimilation of screen level observations, J. Geophys. Res., 114, D08105, doi:10.1029/2008JD011077, 2009. 9648, 9653

Masson, V., Le Moigne, P., Martin, E., Faroux, S., Alias, A., Alkama, R., Belamari, S., Barbu, A., Boone, A., Bouyssel, F., Brousseau, P., Brun, E., Calvet, J.-C., Carrer, D., Decharme, B., Delire, C., Donier, S., Essaouini, K., Gibelin, A.-L., Giordani, H., Habets, F., Jidane, M., Kerdraon, G., Kourzeneva, E., Lafaysse, M., Lafont, S., Lebeaupin Brossier, C., Lemonsu, A., Mahfouf, J.-F., Marguinaud, P., Mokhtari, M., Morin, S., Pigeon, G., Salgado, R., Seity, Y., Taillefer, F., Tanguy, G., Tulet, P., Vincendon, B., Vionnet, V., and Voldoire, A.: The SURFEXv7.2 land and ocean surface platform for coupled or offline simulation of Earth surface variables and fluxes, Geosci. Model Dev. Discuss., 5, 3771–3851, doi:10.5194/gmdd-5-3771-2012, 2012. 9651

Medina, H., Romano, N., and Chirico, G. B.: Kalman filters for assimilating near-surface observations in the Richards equation – Part 3: Retrieving states and parameters from laboratory evaporation experiments, Hydrol. Earth Syst. Sci. Discuss., 9, 13373–13414, doi:10.5194/hessd-9-13373-2012, 2012. 9665

Njoku, E., Jackson, T., Lakshmi, V., Chan, T., and Nghiem, S.: Soil moisture retrieval from AMSR-E, IEEE T. Geosci. Remote, 41, 215–229, 2003. 9647

Noilhan, J. and Mahfouf, J.: The ISBA land surface parameterisation scheme, Global Planet. Change, 13, 145–159, 1996. 9649, 9650

Noilhan, J. and Planton, P.: A simple parameterization of land surface processes for meteorological models, Mon. Weather Rev., 117, 536–849, 1989. 9650

Owe, M., de Jeu, R., and Walker, J.: A methodology for surface soil moisture and vegetation optical depth retrieval using the microwave polarization difference index, IEEE T. Geosci. Remote, 39, 1643–1654, 2001. 9647

Pellarin, T., Calvet, J.-C., and Wagner, W.: Evaluation of ERS scatterometer soil moisture products over a half-degree region in southwestern France, Geophys. Res. Lett., 33, L17401, doi:10.1029/2006GL027231, 2006. 9655

Ragab, R.: Towards a continuous operational system to estimate the root-zone soil moisture from intermittent remotely sensed surface moisture, J. Hydrol., 173, 1–25, 1995. 9647

Design and evaluation at local scale

M. Parrens et al.

Back | Close

Full Screen / Esc

Printer-friendly Version

Interactive Discussion

Reichle, R. H.: Variational assimilation of remote sensing data for land surface hydrologic applications, Ph.D. thesis, Massachusetts Institute of Technology, 2000. 9647

Reichle, R. H. and Koster, R. D.: Bias reduction in short records of satellite soil moisture, Geophys. Res. Lett., 31, L19501, doi:10.1029/2004GL020938, 2004. 9655, 9656, 9665

Reichle, R. H. and Koster, R. D.: Global assimilation of satellite surface soil moisture retrievals into the NASA Catchment land surface model, Geophys. Res. Lett., 32, L02404, doi:10.1029/2004GL021700, 2005. 9647

Rüdiger, C., Calvet, J.-C., Claire, G., Holmes, T., de Jeu, R., and Wagner, W.: An intercomparison of ers-scat and amsr-e soil moisture observations with model simulations over france, J. Hydrometeorol., 10, 431–447, doi:10.1175/2008JHM997.1, 2007. 9655

Sabater, J. M., Jarlan, L., Calvet, J.-C., Bouyssel, F., and de Rosnay, P.: rom near-surface to root-zone soil moisture using different assimilation techniques, J. Hydrometeorol., 8, 194–206, doi:10.1175/JHM571.1, 2007. 9647, 9654, 9666

Saleh, K., Wigneron, J.-P., de Rosnay, P., Calvet, J.-C., and Kerr, Y.: Semi-empirical regressions at L-band applied to surface soil moisture retrievals over grass, Remote Sens. Environ., 101, 415–426, 2006. 9648

Saleh, K., Wigneron, J.-P., Waldteufel, P., De Rosnay, P., Schwank, M., Calvet, J.-C., and Kerr, Y.: Estimates of surface soil moisture under grass covers using L-band radiometry, Remote Sens. Environ., 109, 42–53, 2007. 9648

Schmugge, T. J.: Remote sensing of soil moisture: recent advances, IEEE T. Geosci. Remote, 21, 336–344, 1983. 9647

Schmugge, T. J., Jackson, T. J., and McKim, H. L.: Survey of methods for soil moisture determination, Water Resour. Res., 16, 961–979, doi:10.1029/WR016i006p00961, 1980. 9650

Scipal, K., Holmes, T., de Jeu, R., Naeimi, V., and Wagner, W.: A possible solution for the problem of estimating the error structure of global soil moisture data sets, Geophys. Res. Lett., 35, L24403, doi:10.1029/2008GL035599, 2008. 9656

Shukla, J. and Mintz, Y.: Influence of land-surface evapotranspiration on the earth's climate, Science, 215, 1498–1501, 1982. 9647

Wagner, W., Lemoine, G., and Rott, H.: A method for estimating soil moisture from ERS scatterometer and soil data, Remote Sens. Environ., 70, 191–207, 1999. 9647

Wagner, W., Naeimi, V., Scipal, K., de Jeu, R., and Martínez-Fernández, J.: Soil moisture from operational meteorological satellites, Hydrogeol. J., 15, 121–131, 2007. 9647

Title Page

Abstract | Introduction

Conclusions | References

Tables | Figures

◄ | ►

◄ | ►

Back | Close

Full Screen / Esc

Printer-friendly Version

Interactive Discussion

Walker, J. P. and Houser, P. R.: A methodology for initializing soil moisture in a global climate model: Assimilation of near-surface soil moisture observations, J. Geophys. Res., 106, 11761–11774, doi:10.1029/2001JD900149, 2001. 9647

Table 1. Description of the ISBA-DF experiments. In bold letters, changement in the assimilation experiment with respect to ISBA-DF reference experiment (DF-REF).

Experiment name	assimilation	**B** matrix	CDF	Local precipitation
DF-REF	layer 1	diagonal	three years	yes
DF-H2	**layer 2**	diagonal	three years	yes
DF-B	layer 1	**non diagonal**	three years	yes
DF-CDF	layer 1	diagonal	**yearly**	yes
DF-NP	layer 1	diagonal	three years	**no**

Table 2. w_1 open-loop and analysis scores (r, RMSE, SDD and bias) computed over the 3 yr period. Statistical scores are performed with rescaled observations.

	Experiment	r	RMSE ($m^3 m^{-3}$)	SDD ($m^3 m^{-3}$)	Bias ($m^3 m^{-3}$)
Open-loop	2L	0.69	0.066	0.054	−0.016
	DF-REF	0.79	0.055	0.055	−0.003
Analysis	2L	0.74	0.052	0.037	0.015
	DF-REF	0.87	0.032	0.028	−0.004
	DF-CDF	0.90	0.029	0.025	−0.004
	DF-H2	0.87	0.033	0.020	−0.013
	DF-B	0.88	0.031	0.016	−0.004
	DF-NP	0.86	0.038	0.021	−0.016

Full Screen / Esc

Printer-friendly Version

Interactive Discussion
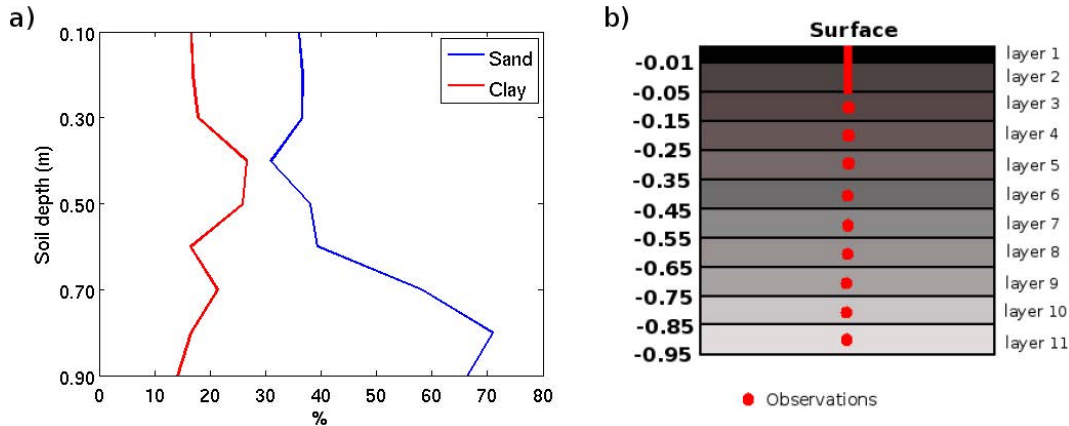
Fig. 1. (a) Sand and clay soil profile (in %) measured at the SMOSREX bare-soil site. **(b)** Soil profile model used with ISBA-DF. The depth of each layer is given in meters. Red dots are places where soil moisture observations were made.
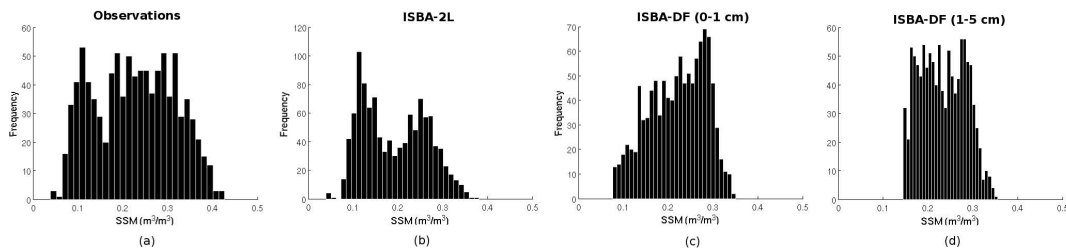
Fig. 2. (a) SSM observations (0–6 cm), **(b)** w_1 modeled by the ISBA-2L LSM, **(c)** w_1 and **(d)** w_2 simulated by ISBA-DF LSM frequency distribution at the SMOSREX site during 2003–2005.
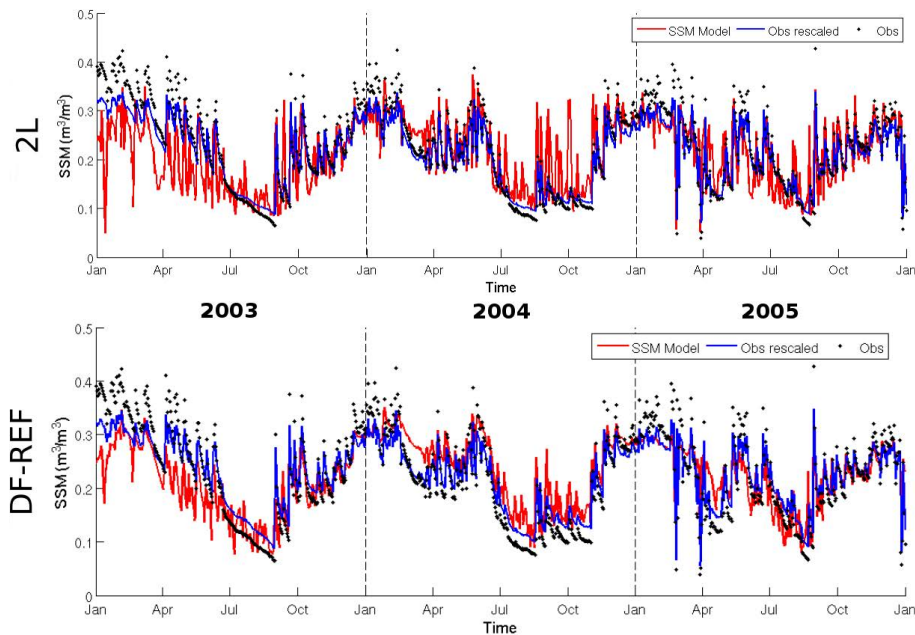
Fig. 3. Time series of SSM observations (black dots), w_1 modeled (red lines) and SSM observations rescaled after CDF matching (blue lines) for ISBA-2L (top) and ISBA-DF (bottom).
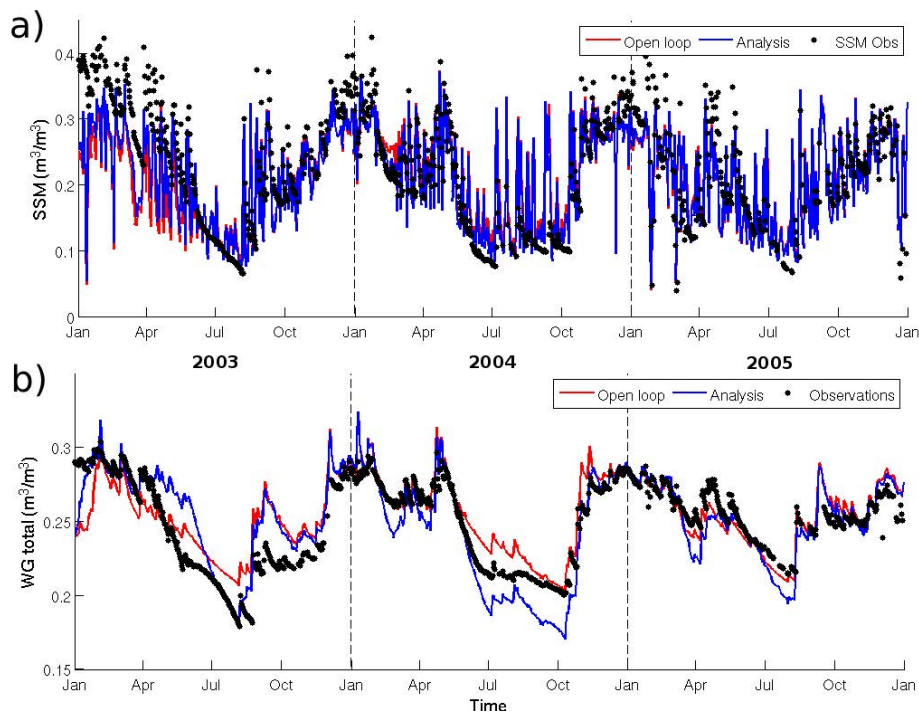
Fig. 4. 2L time series of open loop (red line), analysis (blue line) and SSM observations at the SMOSREX site (black dots) for 2003–2005: in the surface layer **(a)** and in the total reservoir **(b)**. The units are in $\mathrm{m^3\,m^{-3}}$.
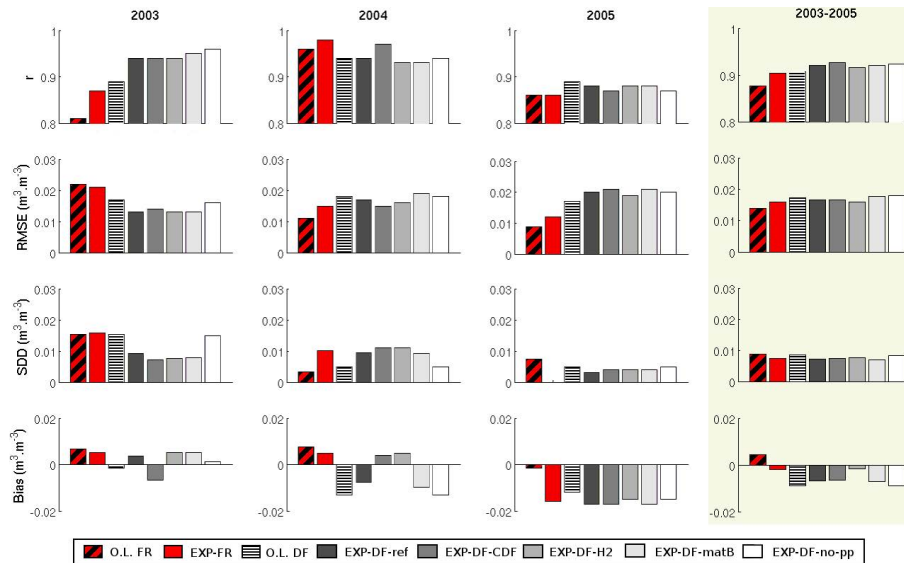
Fig. 5. Yearly and 3 yr period statistical scores for w_{tot} analysis for experiments presented in Table 1 and 2L experiment. O.L. means Open-Loop simulations.
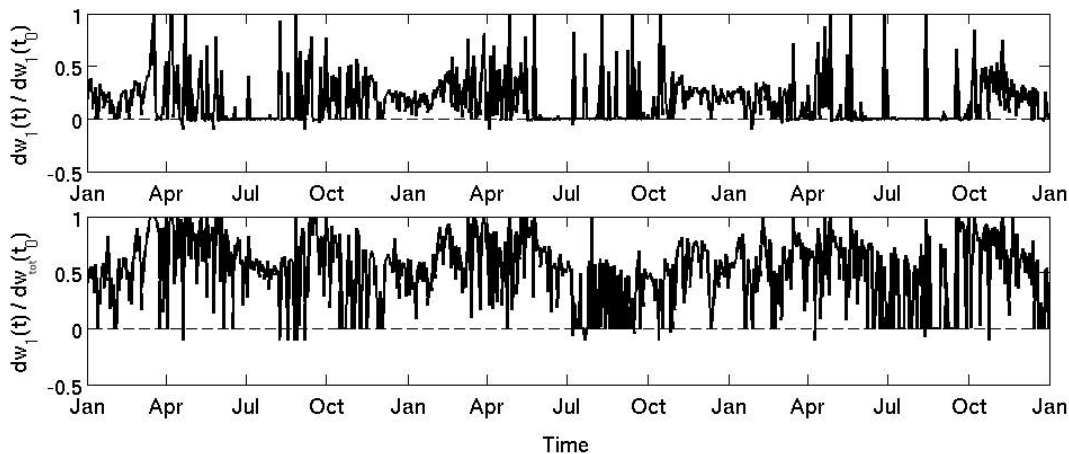
Fig. 6. Time evolution of the two Jacobian terms of ISBA-2L in (top) the first layer and (bottom) the bulk reservoir.

Full Screen / Esc

Printer-friendly Version

Interactive Discussion
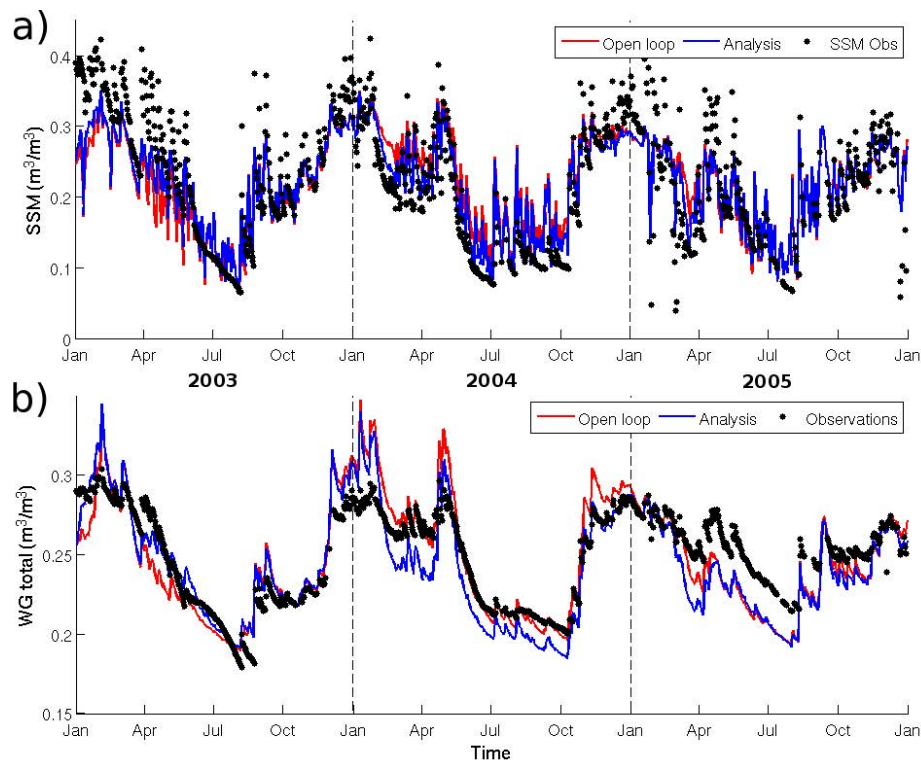
Fig. 7. DF-REF time series of open loop (red line), analysis (blue line) and SSM observations at the SMOSREX site (black dots) for 2003–2005: in the surface layer **(a)** and in the total reservoir **(b)**. The units are in $m^3 m^{-3}$.

Printer-friendly Version

Interactive Discussion
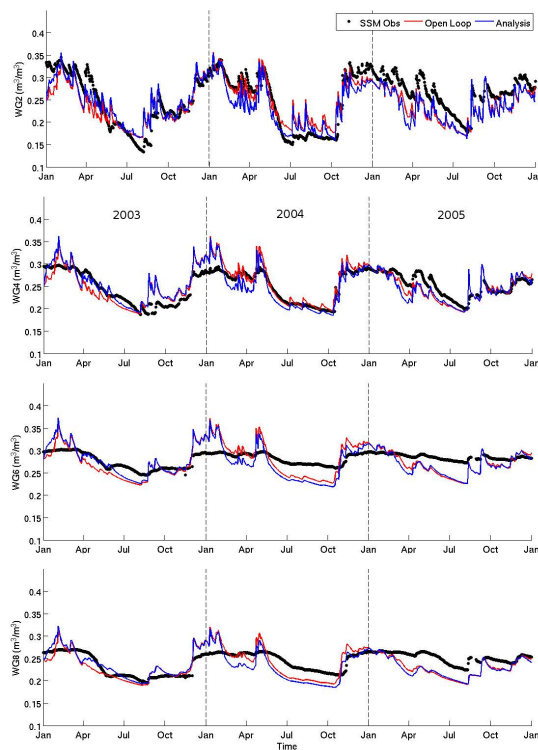
Fig. 8. Time series of soil moisture observations (black dots), soil moisture open-loop (red lines) and soil moisture analysis (blue lines) for four layers: (top) layer 2: 1–5 cm, (top middle) layer 4: 15–25 cm, (bottom middle) layer 6: 35–45 cm and (top) layer 8: 35–45 cm.
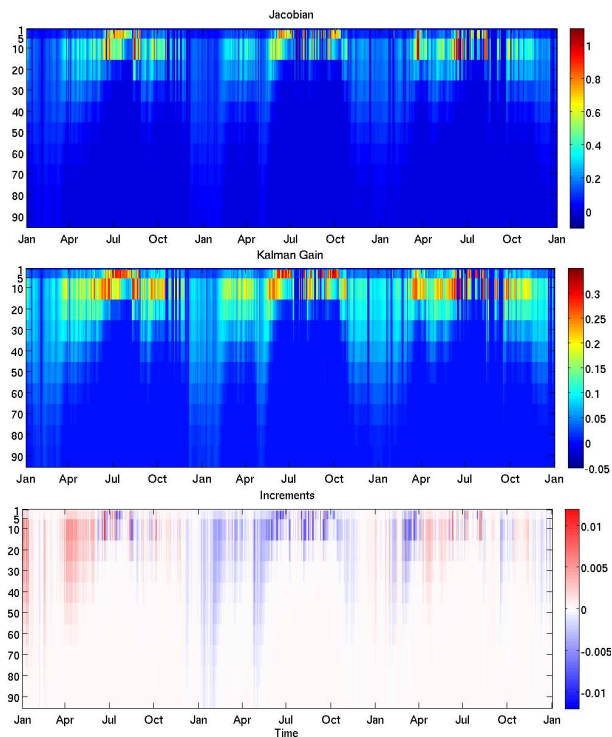
Fig. 9. Representation of the Jacobian (top), the Kalman gain (middle) and increments (bottom) provided of the SSM assimilation for DF-REF. Soil layer depths (in cm) are represented in *y* axis and the time is represented in *x* axis.
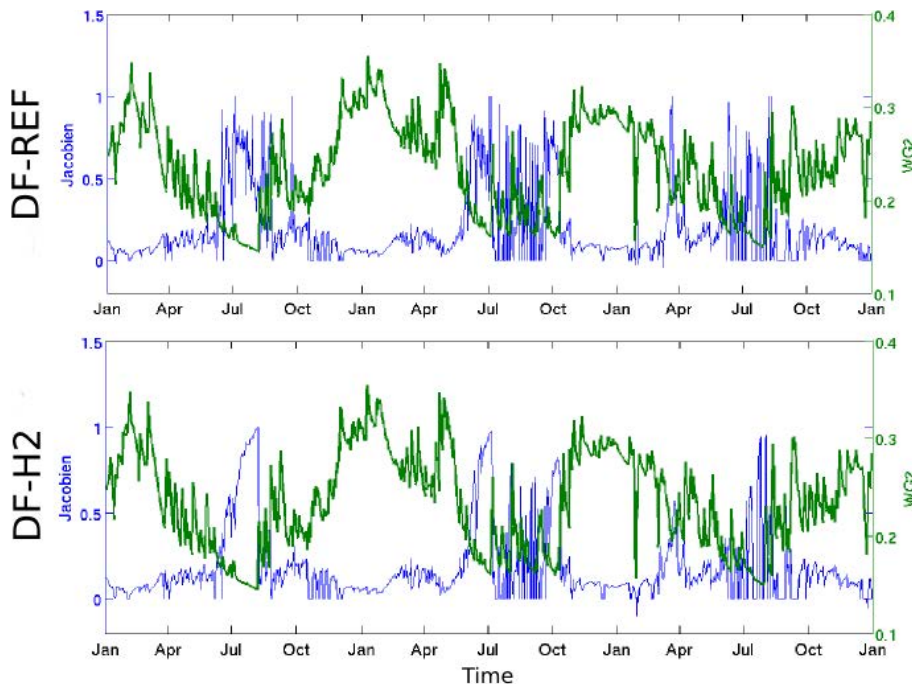
Fig. 10. Time evolution of w_2 using ISBA-DF LSM in the second layer (green line) and the Jacobian values (blue line): (top) $\frac{\partial w_1(t)}{\partial w_2(t_0)}$ in DF-REF and (bottom) $\frac{\partial w_2(t)}{\partial w_2(t_0)}$ in DF-H2.
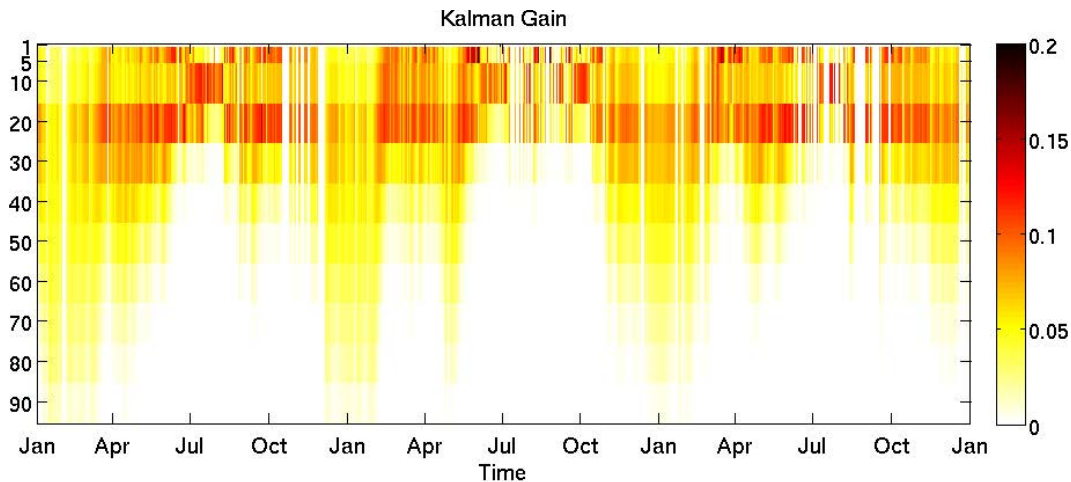
Fig. 11. Difference of the Kalman Gain provided by the SSM assimilation in DF-B and DF-REF. Soil layer depths (in cm) are represented in *y* axis and the time is represented in *x* axis.

Discussion Paper | Discussion Paper | Discussion Paper | Discussion Paper |

HESSD

10, 9645–9688, 2013

Design and evaluation at local scale

M. Parrens et al.

Title Page

Abstract   Introduction

Conclusions   References

Tables   Figures

◄   ►

◄   ►

Back   Close

Full Screen / Esc

Printer-friendly Version

Interactive Discussion
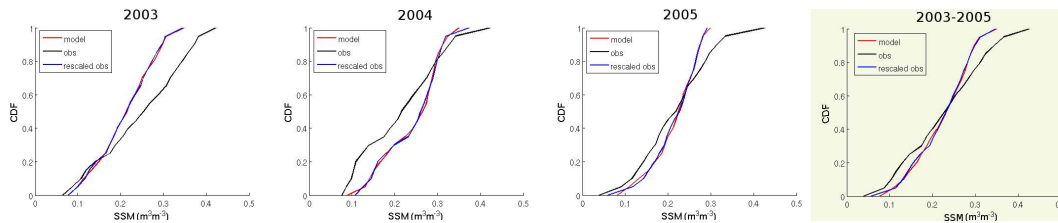
Fig. 12. CDF-matching between w_1 modeled with ISBA-DF LSM and SSM observations for 2003, 2004, 2005 and the 3 yr period.

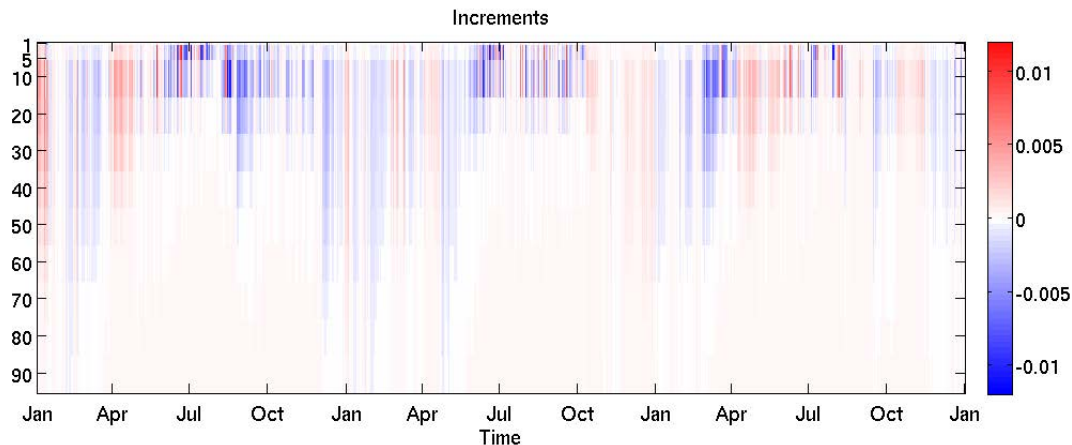**Fig. 13.** Representation of daily increments ($m^3 m^{-3}$) provided by the SSM assimilation in DF-CDF with a year per year CDF matching. Soil layer depths (in cm) are represented on the *x* axis and time on the *y* axis.
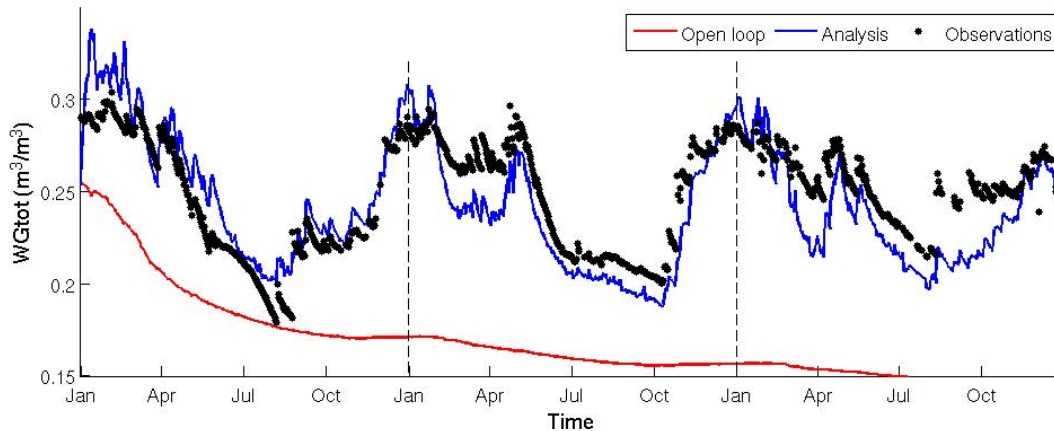
Fig. 14. Time series of root zone soil moisture observations (black dots), soil moisture open-loop simulation (red lines) and soil moisture analysis simulation (blue lines) computed with the expriment DF-NP.